Registration of Images with widely varying Focal Lengths for Quality Inspection of Aircraft Components

Marvin Höhner, Fabian Stoller, Milapji Singh Gill, Alexander Fay
Institute of Automation Technology
Helmut Schmidt University Hamburg
Hamburg, Germany
marvin.hoehner@hsu-hh.de

***Abstract* – Reliable quality inspection of aircraft components to identify defects is an essential process step for maintenance, repair and overhaul (MRO) service providers to ensure safe flight operations. Currently, highly experienced employees inspect and check fine-granular substructure parts of components manually from different perspectives by using a microscope. Methods from image processing and machine learning offer the potential to automate and accelerate this process step without reducing the quality of the inspection. For this purpose, a camera with a wide-angle lens is needed first to capture the entire sub-component. In addition, a microscope camera is required for detailed observation of finer parts and the identification of defects. The aim is to be able to spatially locate the detailed information from the microscope image in an overview image. Accordingly, this overview image can be used by the employee for troubleshooting. In this context image registration is not a trivial task considering the huge difference in focal lengths of both cameras and the corresponding difference in recorded detail. In the following contribution, a two-stage concept for image registration in quality inspection tasks for aircraft components will be presented to overcome this obstacle. An evaluation of this approach was performed using a demonstrator for the inspection of certain aircraft sub-components.**

Keyword – Image Processing, Image Registration, Quality Inspection, Aviation, MRO

I. Introduction

The quality inspection of aircraft components in the field of maintenance to identify defects is an important work step that places considerable demands on the respective MRO-service providers [1]. Highly trained and experienced employees are required for this time-consuming task in order to ensure appropriate quality and the safe functionality of different individual components in flight operation [1, 2]. A variety of line-replaceable units (LRUs) are characterized by a complex structure consisting of several sub-components with fine-granular similar looking parts that must be inspected with utmost attention to detail. Even the smallest deviations can lead to a malfunctioning component. Thus, a thorough quality control and inspection becomes even more important. However, a quality inspection carried out manually by the technician is quite time-consuming. In order to remain competitive and to provide customers with their components quickly and reliably, it could be advantageous to replace this process step by an automated, data-based system. Especially methods from the field of image processing and machine learning offer the potential to assist technicians with these repetitive, time-consuming tasks [2–4].

To ensure reliable detection of defects, images of the sub-components with different levels of magnification and perspectives are required. Microscopically enlarged areas of fine-granular parts are needed for an automated classification of possible defects. Furthermore, similar looking fine-granular parts already examined by the microscope should be located in an overview image with references to faulty points. These are recorded by the second camera with the wide-angle lens showing the whole sub-component. Subsequently, this overview image should be available in a final report, which is needed by the employee for troubleshooting. The transfer of information from a microscopic image to a macroscopic overview image requires that sufficient matching features are found in both images [5]. However, the very large difference in scale in this context represents a significant challenge to be solved in the field of quality inspection of aircraft components.

In the following contribution, a concept is developed which can support MRO service providers in the field of quality inspection of aircraft components in dealing with such challenges as those mentioned above. The concept has been implemented by means of a demonstrator and evaluated at various levels of complexity. The paper is structured as follows: Sec. II briefly describes the quality inspection process of aircraft components as well as elementary methods of image registration. Based on this, functional and non-functional requirements regarding the system setup and the concept are derived. Sec. III discusses related research works covering similar challenges. The two-part concept for the registration of images with varying focal lengths is presented in Sec. IV. Accordingly, Sec. V explains the implementation of the demonstrator with hardware and software components. A discussion in Sec. VI then summarizes the results from the applications that have been carried out at different levels of complexity. Sec. VII provides a final summary of the results and an outlook.

II. Background

A. Quality Inspection of aircraft components

The quality inspection of aircraft components is integrated into an overall process in which the causes of faults are investigated. Typically, the technician examines sub-components with their fine granular parts for possible damages which might be leading to a system failure. When inspecting such subcomponents, the technician looks for anything that deviates visually from a normal state. Depending on the workshop, the entire maintenance process of an aircraft component can be accompanied by one or several different technicians. The maintenance process includes e.g. the receipt, the visual inspection, different tests, the troubleshooting and the final decision on the release of the LRU. A quality inspection can be carried out in different stages of the maintenance process, depending on the degree of disassembly of the component. For sub-components with fine-granular similar looking parts, a microscope is used in most cases. Based on experience, areas that are particularly susceptible to faults are primarily focused on. Typically, the sub-component is inspected from multiple angles. After the inspection a decision has to be made whether a revision is needed or not. This decision is very dependent on the technician and his/her experience. Generally, the inspection of a single sub-component can be completed within a few seconds if there is either a very conspicuous or no defect. However, if cases are involved where the detection is not obvious, the decision-making process can be significantly prolonged. In any case, with several sub-components per LRU, the current process requires a considerable amount of time. On this account, an automated system could be advantageous.

B. Image Registration

Image registration is a method originating in image processing which has been applied to various problems in different domains [6, 7]. It aims to bring two or more images of the same scene taken from different positions, by different cameras or at different time instances into the best possible alignment with each other [8].

Several steps are usually necessary for a successful and precise image registration. For easier processing of the images, a rectification is needed first. Additionally, in order to eliminate the distortion, respective intrinsic camera parameters are required. These are determined by the use of calibration standards [9]. These are for example the focal length of the camera, the horizontal and vertical image size, the location of the focal point in the image plane and the distortion coefficients. Following this step, unambiguous corresponding points are searched for in both images, as far as image sections overlap [5]. These points can be assigned in different ways. A distinction is made between feature-based methods and area-based methods [8, 10]. In feature-based methods, a set of features is first extracted from both images before an attempt is made to assign them to each other [8]. Area-based methods combine the feature recognition step with finding corresponding points [10]. After finding enough corresponding points in the images, this can be used to determine a transformation matrix between these images. The number of corresponding points required depends on the complexity of the required transformation. The more points can be included in the calculation, the more precise the transformation will be. Once solved, this matrix can be used to assign any pixel from an image to the other one [5].

C. Requirements

For the specific task of image registration in the quality inspection of aircraft components, functional and non-functional requirements are gathered with regard to the concept to be developed. The requirements are divided into two subsets. The first set of functional and non-functional requirements (see TABLE I*)* addresses the system structure. These are derived from the designed overall system, its objectives as well as an observation from the process described above. The objective here is to select the relevant hardware and software components for the task of image registration and the targeted subsequent automated quality inspection (not part of this contribution).

TABLE I: FUNCTIONAL AND NON-FUNCTIONAL REQUIREMENTS.

ID	*Category*	*Requirement*
F-1	Functional	The system requires a microscope camera and a wide-angle camera to record the sub-component in various degrees of detail.
F-2	Functional	The system requires two cameras that are in a fixed position relative to each other so that the relative position of the cameras remains constant between shots.
F-3	Functional	The image section of the microscope camera must be in the image section of the wide-angle camera so that the same fine-granular part of a sub-component can be captured in both images.
F-4	Functional	The wide-angle camera must be able to record 24 images per second so that each image from the microscope camera can be assigned to the wide-angle camera.
F-5	Functional	Images taken in the same time period must be able to be matched to each other to ensure that both images depict the same scene.
F-6	Functional	The cameras must be adjustable by up to 45 degrees in any direction so that the fine-granular parts can be viewed from the side.
F-7	Functional	The working distance to the subcomponent is 100 mm, so that even subcomponents with high structures can be viewed.
F-8	Functional	The stand must be 100 mm adjustable in height so that fine-granular parts can be viewed at different heights.
NF-1	Non-Functional	The microscope camera must magnify the image 30 times in order to perform a quality inspection of fine-granular parts
NF-2	Non-Functional	The wide-angle camera must have a minimum aperture angle of 110.8 degrees so that an overview image of the sub-component can be taken.
NF-3	Non-Functional	The wide-angle camera must display 1mm x 1 mm with at least 5x5 pixels so that details can be recognized.

The second set (see TABLE II) exclusively deals with non-functional requirements, which are to be considered and evaluated in particular for the image registration concept to be developed.

TABLE II: FUNCTIONAL AND NON-FUNCTIONAL REQUIREMENTS.

ID	*Category*	*Requirement*
NF-4	Non-Functional	The system should be able to detect at least the area that the microscope camera has already observed.
NF-5	Non-Functional	It must be possible to freely hold the subcomponent under the camera in order to increase acceptance among employees.
NF-6	Non-Functional	The system should be functional regardless of the type of subcomponent.

III. RELATED WORKS

According to [11], image registration consists of five stages: Feature detection and description, feature matching, rejection of outliers, estimation of a transformation and the reconstruction of the view. The state-of-the-art feature detectors (e.g. [10, 12–14]) all come with their own descriptors. The aim here is to describe features independently from scale, rotation and affine transformation. There are, nonetheless, limitations to this claim which become obvious when registering images with hugely different spatial resolutions.

A more recently developed feature detector and descriptor is KAZE [10]. It uses nonlinear scale spaces to locally adapt the blur to the image data and reduce image noise while keeping object boundaries at the same time. This yields a higher localization accuracy. It is also invariant to rotation.

In the field of remote sensing the registration of images from different modalities like infrared or radar with different properties and resolutions is a typical challenge. The methods employed have evolved from manual point matching to automated feature-based matching and estimation of the transform [6]. The authors of [6] outline that the use of image features derived from convolutional neural network (CNN) hidden layers may yield results that are superior to the SIFT [12] features that are widely used. Albeit, the authors emphasize as well that the use of CNNs leads to challenges like the availability of training data. Especially during the quality inspection of aircraft components in the way described, tasks with a low quantity of defects on the one hand and high product variations on the other hand this is a problem.

An application that also employs a registration between cameras with vastly different properties is the registration of the field of view (FOV) of pan-tilt-zoom (PTZ) surveillance cameras onto aerial orthophotos like it is presented in [7]. The authors propose a method that is feature-based without disclosing the actual algorithm used. However, the field of view of each camera in a surveillance system is transformed onto a map-like orthophoto to simplify handling of the different cameras by users.

Basically, looking at the related works, it can be observed that a comparable approach to the one in this contribution could not be found. This may be due to the very specific requirements that have to be considered in this field. Nevertheless, the approach presented in this contribution could also be helpful for use cases in other domains (e.g. medicine).

IV. CONCEPT FOR IMAGE REGISTRATION IN QUALITY INSPECTION OF AIRCRAFT COMPONENTS

With those challenges and requirements in mind a novel method for bridging the difference in focal lengths has been developed. The approach consists of two steps in order to register the images of a microscopic camera onto a macroscopic image containing the complete part under scrutiny.

A. *Two Step Concept*

Preliminary tests have shown that the direct registration from the microscopic camera onto the macroscopic wide-angle overview image seems hardly possible. Therefore, an intermediate image with an intermediate magnification is introduced. The camera capturing this intermediate image and the microscope camera are in fixed relative positions. Accordingly, only their joint relative position with respect to the object may vary. The microscopic camera with a nearly telecentric lens, however, has a very narrow window where the images captured are sufficiently sharp for further image processing. Consequently, the distance of the object, the sub-component under inspection, from the cameras is assumed to be nearly constant. The position of the microscope camera's FOV in relation to the coordinates of the intermediate camera can be determined by matching key points of a known calibration pattern. We used the corner points of a checkerboard pattern visible in both cameras images to determine a transformation between the coordinates of the two cameras.

Subsequently, the second step is the registration of the image taken by the intermediate camera onto the overview image of the complete part under investigation that has been taken before the inspection. This can be conducted using the state-of-the-art in feature-based image registration. Further preliminary tests with the state-of-the-art feature detectors and descriptors SIFT [12], BRISK [15] and KAZE [10] have shown that KAZE features have a superior performance in preliminary experiments with regard to the requirements.

B. *Transformation Matrix M1*

The first step of the two-step registration method is conducted before the actual inspection. The matrix $M1$ describes the transformation from coordinates of the microscopic camera to the coordinates of the intermediate camera. It should be mentioned that $M1$ is constant due to the likewise constant relative positions of the cameras. As long as the internal camera parameters (such as focus or magnification) or the relative position of the cameras to each other are not changed, recalibration is not necessary.

As the intermediate camera is a wide-angle camera with a rather short focal length, the image captured underlies rather intensive distortion by the camera's optics. In order to undistort the images, a single camera calibration is performed using an asymmetric checkerboard pattern as well (see [16]). The microscopic camera does not need to be undistorted because of its telecentric optics. After the wide-angle camera's images have been undistorted, an asymmetric checkerboard pattern is placed in the FOV of the microscopic camera and the wide-angle camera at the same time. The corner points of the checkerboard fields are determined as corresponding points in both views and subsequently used for estimating the transformation $M1$. The complete procedure for the computation of $M1$ is described in FIGURE 1.

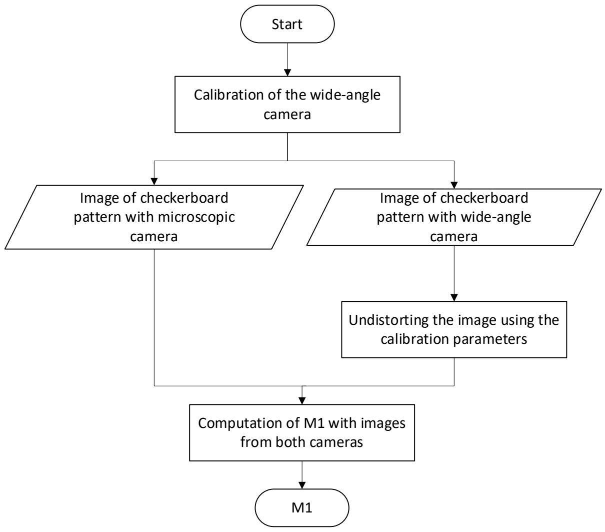

FIGURE 1: FLOW DIAGRAM OF THE PROCEDURE FOR ESTIMATING M1.

C. *Transformation Matrix M2*

For the registration of images from the wide-angle camera with the overview image, taken before the inspection process, a feature-based approach to calculating the transformation matrix $M2$ is chosen. With the Matrix $M2$ a transformation of coordinates from the wide-angle camera into the overview image's coordinate system is enabled. As mentioned before, preliminary experiments yield that KAZE is the most suitable feature detection and description algorithm from the state-of-the-art. In these preliminary tests it exhibits a considerably more reliable registration than SIFT and BRISK. For detecting and rejecting outliers from the set of matched features between the two images MSAC [17] is employed. After outlier rejection the remaining inliers are used for an estimation of the transformation matrix $M2$. This transformation needs to be calculated for every newly taken image. This is due to the fact that the position of the sub-component will change between images when held by a person. Consequently, the same applies to $M2$.

The complete transformation of the points in the microscopic camera's images onto the overview image taken of the whole sub-component before the actual inspection is thus a subsequent application of $M1$ and $M2$. In this regard $M1$ is being fixed during the inspection and $M2$ is changing with every image taken. Using these transformations, the areas and even single fine-granular and similar-looking parts found to be faulty can be marked in the overview image.

V. IMPLEMENTATION

Based on the preliminary considerations described, the implementation of the demonstrator, consisting of hardware and software components, is described below. In this context, the functional requirements F-1 to F-8 and the non-functional requirements NF-1 to NF-3 are considered (see TABLE II and II).

A. Hardware

The algorithm described in the previous section has been implemented in a semi-automated inspection system for quality inspection. FIGURE 2 depicts the overall system. The most important detail of the implementation is that the cameras are mounted in a parallel position. Also, they should be mounted as close to each other as possible. Both helps to minimise errors caused by deviations of the object from its assumed constant distance to the cameras.

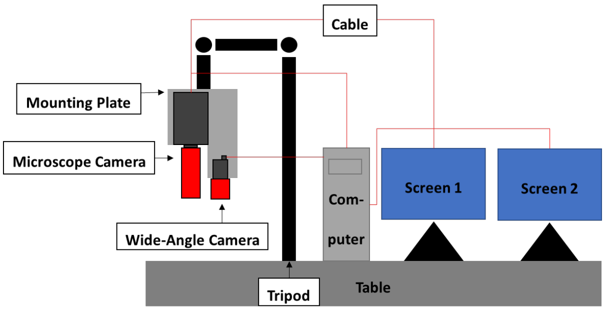

FIGURE 2 OVERVIEW OF THE SYSTEM SETUP WITH TWO CAMERAS AND TWO DISPLAYS.

The microscopic camera uses a Gigabit Ethernet connection for data transfer and the wide-angle camera is interfaced using USB. Both have their own monitor for displaying the current image feed or the accumulated information gathered for simplifying the inspection for tiny faults. The working distance of the microscopic camera is $100mm$ and the wide-angle camera has a minimal working distance of $37mm$, respectively. The resolution of the wide-angle camera is chosen so that it resolves small details sufficiently. This also supports the stereo calibration of the two cameras by displaying the calibration points with higher precision. The calibration itself is conducted using an 8x7 checkerboard with squares of $2mm$ width and height each. The components have been chosen in order to fulfil the requirements described earlier.

B. Software

On the basis of these hardware components the two-step algorithm for registering the microscopic camera with an overview image taken of the complete part under inspection has been implemented using MATLAB 2021b. The cameras are interfaced using their respective Python-based APIs so that the prototypical implementation does not run online. Because especially the microscopic camera has only a narrow region where it produces sharp images, NIQE [18] is used as an image quality metric to filter out images of insufficient quality before the actual registration process [19].

VI. DISCUSSION

The system presented must meet the requirements discussed previously. Therefore, the demonstrator has been tested at three different levels of complexity. This aims to verify whether the system meets the performance-related requirements NF-4 and NF-5. Furthermore, the performance of the two-stage concept is to be evaluated. Performance in this context is assessed using the deviation of test points transformed from the microscopic image to the overview image from the real points in the overview image. The ground truth positions of points in the overview image have been determined manually. As a test object an artificial geometric pattern printed on a rigid board has been used to mimic an aircraft component. The board has test points distributed all over it. The test board is displayed in FIGURE 3. For a final evaluation an actual component with similar-looking fine-granular parts has been used.

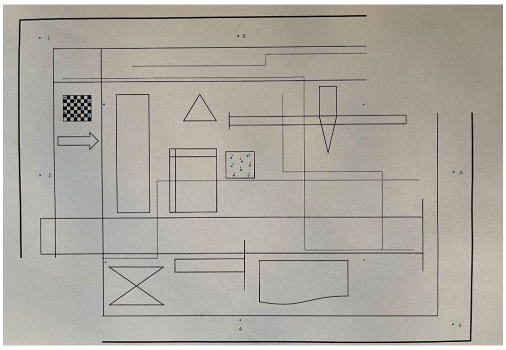

FIGURE 3 TEST BOARD WITH GEOMETRIC PATTERNS AND DISTRIBUTED TEST POINTS.

A. Evaluation using a static perpendicular scene

The first tests are conducted with a static setup. Consequently, the test board remains in a fixed position during image capture. The position of the test object is approximately perpendicular in front of the two cameras. The system is set up in a way that the cameras can capture sharp images of the test object. The wide-angle camera is calibrated and the transformation $M1$ is computed in compliance with FIGURE 1 before the actual image capturing. The test board is captured in several different but static positions.

TABLE III shows the overall results from those experiment. The proposed two-step algorithm exhibits a mean error of $0.8377px$ and a standard deviation of the error of $0.4220px$ in the wide-angle images. Here, $6.5px$ correspond to a distance of $1mm$. Also, TABLE III demonstrates qualitatively that the errors resulting from each step of the registration are not oriented equally. In FIGURE 4 the steps of the registration of the test points are displayed using 3 images. In the result image on the right the error of the registration is illustrated with blue circles showing the assumed ground truth and the red dots showing the estimated location. The total error is, hence, not significantly larger than the errors in each of the two steps. The overall error is sufficiently small with respect to the distribution of the fine-granular parts. It is in the submillimetre range depending on the distance from which the overview image is taken in a particular case. Consequently, it is possible to mark single fine-granular parts found in the microscopic camera in the overview image with considerable accuracy. Accordingly, NF-4 is fulfilled to a high degree.

FIGURE 4 EVALUATION OF THE PRECISION OF THE REGISTRATION USING A TEST PATTERN.

TABLE III: ERRORS OF THE CALCULATED MATRICES M1, M2 AND THE OVERALL TRANSFORMATION M1*M2 WITH THE TEST OBJECT LYING ON A TABLE.

Error E	$M1$	$M2$	$M1$ & $M2$
Mean error μ_e in px	0.8377	0.6779	0.9065
Standard deviation of the error σ_e in px	0.4220	0.3436	0.4756
Maximum error E_{max} px	2.1656	1.7457	2.2273

B. Evaluation with varying distance

The second level of the evaluation focusses on the error when varying the distance of the test board from the cameras. This distance is assumed to be constant so that $M1$ does not need to be recalculated for every image.

The results in TABLE VI show the measured errors with the test board at different distances. Deviations are setup in a range of $-5mm$ to $5mm$ from the optimal distance of $100mm$ from the microscopic camera. As expected, the errors increase with increasing deviation from the optimal working point. The errors increase faster when increasing the distance from the camera as compared to decreasing the distance. Also, the relatively constant distribution of the error around its mean confirms that this is a systematic error.

The use of NIQE [18] for image quality estimation assesses only images taken within a range of $-1mm$ to $2mm$ as sufficient for further processing. For this distance, the mean errors are $2.9059px$ and $4.6809px$, respectively. This is equivalent to a total deviation from the ground truth of less than $1mm$ as measured on the test board in the wide-angle image. These findings support that the requirement NF-4 is fulfilled. And even more so, because it is possible to not only mark the region but even fine-granular parts in the overview image with considerable accuracy.

TABLE VI: ERROR RESULTING FROM THE VARIATION OF THE DISTANCE OF THE OBJECT FROM THE CAMERA.

Deviation from focal distance in mm	Mean error μ_e in px	Standard deviation σ_e in px	Maximum error in px
-5	12.7711	0.9267	14.9429
-4	9.5361	0.9119	11.5441
-3	7.5892	0.8924	8.9504
-2	5.0119	0.8963	6.8827
-1	2.9059	0.6796	3.9016
0	0.8377	0.4220	2.1656
1	2.2301	0.7510	3.9643
2	4.6809	0.8743	5.9602
3	6.2440	0.9505	7.8922
4	8.3654	1.4619	10.3148
5	11.7280	1.0494	13.0224

C. Evaluation of a manual part inspection

The final stage of the evaluation aims to replicate conditions during a real inspection of a potentially faulty part. Therefore, several continuous images are captured. In this sequence of images, an actual component with fine-granular similar-looking parts has been used as test object. The test part is positioned manually in the FOV of both cameras like it would be done during an actual inspection process. The images are therefore prone to motion blur and other insufficiencies resulting from human motion and imprecision in positioning the part.

TABLE V shows the resulting precision of the registration. The mean overall error when transforming test points from the microscopic view onto the overview is $\mu_E = 1.6023px$. Even the resulting maximum error $E_{max} = 3.2669px$ on the overview image in terms of distance is, however, still well below $1mm$ for both test objects. The absolute errors are slightly greater than those observed in the first two stages using the test board. The general distribution of the error, however, is very comparable to the experiments using the test board. Therefore, these results demonstrate compliance of the developed system to the requirements NF-4, NF-5 and even NF-6 because the proposed method is able to localize fine-granular parts in the overview for an actual part that is guided by hand and also in the geometric pattern.

TABLE V: ERRORS OF THE CALCULATED MATRICES M1, M2 AND THE OVERALL TRANSFORMATION M1*M2 FOR THE MANUAL POSITIONING WITHOUT GUIDANCE.

Error E	$M1$	$M2$	$M1 * M2$
Mean error μ_E in px	1.4320	0.8348	1.6023
Standard deviation of the error σ_E in px	0.6671	0.3987	0.8157
Maximum error E_{max} px	2.4992	1.7861	3.2669

VII. SUMMARY AND OUTLOOK

In the present contribution a method has been described to bridge the gap between cameras with widely varying focal lengths. This difference has proven to be a challenge for image registration. Especially quality inspection tasks of aircraft components manually or automated may benefit from the two-step solution. It allows to accumulate the information gained from highly detailed microscopic images on a macroscopic overview image with a wide-angle image as an intermediate step. In the practical evaluation of the method its accuracy has been demonstrated. Even under challenging circumstances with an actual person holding the component, the method demonstrated an accuracy that is high enough for localizing fine-granular parts from the microscopic imagery on the overview image. With regard to the requirements mentioned in the beginning, most of them have been fulfilled by selecting suitable components. For the requirements NF-4, NF-5 and NF-6 compliance has been demonstrated by the experiments presented.

With this two-step algorithm manual inspection tasks of aircraft components may be supported by decreasing the amount of overhead for documentation and reporting necessary to track the deficiencies. A more thorough investigation of suspicious regions of the inspected parts is made possible by the increased amount of time available to the inspection worker. Due to faster inspection and documentation, this system is a first step towards the full automation of such manual inspection tasks. With the ability to locate the currently inspected components on the part, automated inspection systems may infer where to look for defects and fix them if possible. For future research it would be interesting if this two-step approach could be further simplified by the use of a deep learning approach rather than a classic image processing pipeline as described.

ACKNOWLEDGEMENT

This paper is funded by dtec.bw – Digitalization and Technology Research Center of the German Federal Armed Force [ProMoDi].

REFERENCES

[1] C. Beltran-Gonzalez, M. Bustreo, and A. Del Bue, "External and internal quality inspection of aerospace components," in *2020 IEEE International Workshop on Metrology for AeroSpace: Virtual conference, 22-24 June 2020 : proceedings*, Pisa, Italy, M. Marracci and A. Buffi, Eds., 2020, pp. 351–355, doi: 10.1109/MetroAeroSpace48742.2020.9160103.

[2] S. Martelli *et al.,* "Deep Endoscope: Intelligent Duct Inspection for the Avionic Industry," *IEEE Trans. Ind. Inf.*, vol. 14, no. 4, pp. 1701–1711, 2018, doi: 10.1109/TII.2018.2807797.

[3] M. Heizmann *et al.,* "Implementing machine learning: chances and challenges," *at - Automatisierungstechnik*, vol. 70, no. 1, pp. 90–101, 2022, doi: 10.1515/auto-2021-0149.

[4] Y. D. Yasuda, F. A. Cappabianco, L. E. G. Martins, and J. A. Gripp, "Aircraft visual inspection: A systematic literature review," *Computers in Industry*, vol. 141, p. 103695, 2022. doi: 10.1016/j.compind.2022.103695. [Online]. Available: https://www.sciencedirect.com/science/article/pii/S0166361522000926

[5] R. Szeliski, *Computer Vision: Algorithms and Applications* (SpringerLink Bücher). London: Springer London, 2011.

[6] S. Dawn, V. Saxena, and B. Sharma, "Remote Sensing Image Registration Techniques: A Survey," in 2010, pp. 103–112, doi: 10.1007/978-3-642-13681-8_13.

[7] J. W. Davis, "Camera Control and Geo-Registration for Video Sensor Networks," in *Distributed Video Sensor Networks*, B. Bhanu, Ed., London: Springer London Limited, 2011, pp. 247–257. [Online]. Available: https://link.springer.com/chapter/10.1007/978-0-85729-127-1_17

[8] B. Zitová and J. Flusser, "Image registration methods: a survey," *Image and Vision Computing*, vol. 21, no. 11, pp. 977–1000, 2003, doi: 10.1016/S0262-8856(03)00137-9.

[9] Z. Zhang, "Flexible camera calibration by viewing a plane from unknown orientations," in *The proceedings of the Seventh IEEE International Conference on Computer Vision: September 20 - 27, 1999, Kerkyra, Greece*, Kerkyra, Greece, 1999, 666-673 vol.1, doi: 10.1109/ICCV.1999.791289.

[10] P. F. Alcantarilla, A. Bartoli, and A. J. Davison, "KAZE Features," in 2012, pp. 214–227, doi: 10.1007/978-3-642-33783-3_16.

[11] S. A. K. Tareen and Z. Saleem, "A comparative analysis of SIFT, SURF, KAZE, AKAZE, ORB, and BRISK," in *2018 International Conference on Computing, Mathematics and Engineering Technologies (iCoMET)*, 2018, doi: 10.1109/icomet.2018.8346440.

[12] D. G. Lowe, "Distinctive Image Features from Scale-Invariant Keypoints," *International Journal of Computer Vision*, vol. 60, no. 2, pp. 91–110, 2004. doi: 10.1023/B:VISI.0000029664.99615.94. [Online]. Available: https://link.springer.com/article/10.1023/b:visi.0000029664.99615.94

[13] P. Alcantarilla, J. Nuevo, and A. Bartoli, "Fast Explicit Diffusion for Accelerated Features in Nonlinear Scale Spaces," in *Procedings of the British Machine Vision Conference 2013*, 2013, doi: 10.5244/c.27.13.

[14] H. Bay, T. Tuytelaars, and L. van Gool, "SURF: Speeded Up Robust Features," in *Computer vision - ECCV 2006: 9th European Conference on Computer Vision, Graz, Austria, May 7 - 13, 2006; proceedings* (Lecture notes in computer science 3951), A. Leonardis, H. Bischof, and A. Pinz, Eds., Berlin: Springer, 2006, pp. 404–417.

[15] S. Leutenegger, M. Chli, and R. Y. Siegwart, "BRISK: Binary Robust invariant scalable keypoints," in *2011 International Conference on Computer Vision*, 2011, doi: 10.1109/iccv.2011.6126542.

[16] Z. Zhang, "A flexible new technique for camera calibration," *IEEE Trans. Pattern Anal. Machine Intell.*, vol. 22, no. 11, pp. 1330–1334, 2000, doi: 10.1109/34.888718.

[17] P. Torr and A. Zisserman, "MLESAC: A New Robust Estimator with Application to Estimating Image Geometry," *Computer Vision and Image Understanding*, vol. 78, no. 1, pp. 138–156, 2000, doi: 10.1006/cviu.1999.0832.

[18] A. Mittal, R. Soundararajan, and A. C. Bovik, "Making a "Completely Blind" Image Quality Analyzer," *IEEE Signal Process. Lett.*, vol. 20, no. 3, pp. 209–212, 2013, doi: 10.1109/lsp.2012.2227726.

[19] M. Höhner, "Konzeptionierung und Implementierung einer Pipeline zu qualitätsbasierten Auswahl von Einzelbildern aus einem fortlaufenden Strom an Bildern," Laboratory Project, Helmut Schmidt University/University of the Federal Armed Forces, Hamburg, 2022.